Cell Motility and the Cytoskeleton 52:97–106 (2002)

Micropatterning Tractional Forces in Living Cells

Ning Wang,[1]* Emanuele Ostuni,[2] George M. Whitesides,[2] and Donald E. Ingber[3]

[1]*Physiology Program, Harvard School of Public Health, Boston, Massachusetts*
[2]*Department of Chemistry and Chemical Biology, Harvard University, Cambridge, Massachusetts*
[3]*Departments of Surgery and Pathology, Children's Hospital and Harvard Medical School, Boston, Massachusetts*

Here we describe a method for quantifying traction in cells that are physically constrained within micron-sized adhesive islands of defined shape and size on the surface of flexible polyacrylamide gels that contain fluorescent microbeads (0.2-μm diameter). Smooth muscle cells were plated onto square (50 × 50 μm) or circular (25- or 50-μm diameter) adhesive islands that were created on the surface of the gels by applying a collagen coating through microengineered holes in an elastomeric membrane that was later removed. Adherent cells spread to take on the size and shape of the islands and cell tractions were quantitated by mapping displacement fields of the fluorescent microbeads within the gel. Cells on round islands did not exhibit any preferential direction of force application, but they exerted their strongest traction at sites where they formed protrusions. When cells were confined to squares, traction was highest in the corners both in the absence and presence of the contractile agonist, histamine, and cell protrusions were also observed in these regions. Quantitation of the mean traction exerted by cells cultured on the different islands revealed that cell tension increased as cell spreading was promoted. These results provide a mechanical basis for past studies that demonstrated a similar correlation between spreading and growth within various anchorage-dependent cells. This new approach for analyzing the spatial distribution of mechanical forces beneath individual cells that are experimentally constrained to defined sizes and shapes may provide additional insight into the biophysical basis of cell regulation. Cell Motil. Cytoskeleton 52:97–106, 2002.

Key words: cell shape; cell mechanics; microfabrication; traction force microscopy; flexible gel

INTRODUCTION

Micropatterning of adherent cells using microfabricated culture substrates is a powerful experimental tool for studying the effect of cell shape on cell functions, including proliferation, differentiation, apoptosis, and motility [O'Neill et al., 1986; Singhvi et al., 1994; Chen et al., 1997; Baill et al., 1998; Dike et al., 1999]. For example, cells can be switched between growth and death programs by varying the size of the extracellular matrix (ECM)-coated adhesive island to which a cell can adhere [Chen et al., 1997]. In general, growth increases in parallel as the island area is increased and cell spreading is promoted, whereas apoptosis is observed in cells on the smallest islands. Based on the observation that cell growth correlated more closely with the extent of cell spreading than the total area of ECM contact, it was suggested that the shape of the adhesive island impacts on cell behavior as a result of cell distortion and associated changes in the cellular mechanical force balance

Contract grant sponsor: NASA; Contract grant sponsor: NIH; Contract grant numbers: NAG2-1509, HL65371, HL33009, GM30367, CA45548; Contract grant sponsor: Harvard's MRSEC.

Emanuele Ostuni's present address is Surface Logix, Inc., 50 Soldier's Field Place, Brighton, MA 02135.

*Correspondence to: Dr. Ning Wang, Physiology Program, Harvard School of Public Health, 665 Huntington Ave., Boston, MA 02115. E-mail: nwang@hsph.harvard.edu

Received 20 December 2001; Accepted 14 February 2002

Published online in Wiley InterScience (www.interscience.wiley.com). DOI: 10.1002/cm.10037

[Chen et al., 1997]. However, this remains to be demonstrated directly.

Thus, the primary goal of the present study was to develop a method whereby we could quantitate mechanical forces exerted by individual cells that were physically constrained to specific sizes and shapes on the micron scale. This was accomplished by combining and modifying two published techniques: a membrane patterning technique (MEMPAT) for shaping cells [Ostuni et al., 2000] and a traction microscopy method for quantitating tractional forces beneath single cells in culture [Pelham and Wang, 1997].

MEMPAT uses microengineered elastomeric membranes with through-holes of precise size and shape (e.g., micron-sized squares or circles) that can be conformally sealed onto culture surfaces, such as glass or plastic [Ostuni et al., 2000]. ECM molecules may be applied exclusively to the small regions exposed by the holes and then, after the membrane is peeled off, cells adhere preferentially to the ECM-coated islands and not to the surrounding non-adhesive regions of the substrate. Alternatively, the substrate can be pre-coated to make its entire surface adhesive before overlying the elastomeric membrane. In this case, cell adhesion is restricted exclusively to the regions exposed by holes in the membrane. When the membrane is removed, the adherent cells are then released from their shape constraints, thus permitting analysis of cell spreading and movement onto the surrounding ECM-coated substrate.

In traction force microscopy, living cells are cultured on flexible polyacrylamide gels that contain fluorescent microbeads (0.2-μm diameter) directly beneath the surface of the gel [Pelham and Wang, 1997]. The motion of these beads can be tracked in the vicinity of attached cells, and the resulting displacement field can be measured to determine the mechanical strain induced in the gel by the overlying cells. Algorithms that calculate tractions that arise from the cell-substrate mechanical interaction allow quantitation of these forces as well as analysis of their spatial distribution beneath individual cells [Dembo and Wang, 1999; Butler et al., 2002].

In the present study, we combined the above two methods and found that cell tractional forces could be clearly visualized within localized regions of the gel directly beneath cells cultured on individual adhesive islands. Use of this approach revealed a direct correlation between cell spreading and mean cell traction.

MATERIALS AND METHODS

Cell Culture

Human airway smooth muscle (HASM) cells were isolated and passaged 3–7 times according to previous protocols [Panettierri et al., 1989]. Confluent cells were serum-deprived for 48 h prior to plating overnight in serum-free medium on polyacrylamide gels patterned with type I collagen (0.2 mg/ml).

Polyacrylamide Gels

Flexible polyacrylamide gels were created by adapting a published technique [Pelham and Wang, 1997]. The gels were polymerized after 0.2-μm diameter fluorescent beads were added [Wang et al., 2002]. A 12-mm (or 22-mm) diameter gel was made on each 35-mm dish (or 45 × 55 mm cover glass).

The polyacrylamide gels fabricated in this manner were determined to be about 70 μm thick using confocal microscopy, and found to have superb optical quality for observation of fluorescence at high magnification. The gels have nearly ideal elastic behavior, and their flexibility can be controlled by changing the relative concentration of acrylamide and bis [Pelham and Wang, 1997]. The Young's modulus of the polyacrylamide gels used in this study (0.25% bis and 2% acrylamide) was estimated to be 1,300 Pa using the method described in Wang et al. [2002].

PDMS Membrane Preparation and Modification

Polydimethylsiloxane (PDMS) membranes were fabricated according to the MEMPAT procedures described earlier [Ostuni et al., 2000; Duffy et al., 1999; Jackman et al., 1999]. Briefly, masters containing raised features of photoresist in the desired shape (e.g., square or round posts, 25 or 50 μm in diameter) were generated using photolithography. The masks used in the photolithographic step were printed on transparency film with a high resolution printer using a previously described rapid prototyping technique [Qin et al., 1996].

The PDMS prepolymer (Dow Corning, Sylgard 184) was spin-coated on the raised features of photoresist to a thickness lower than the height of the posts. This procedure created a thin film of PDMS, with menisci around the photoresist posts [Jackman et al., 1999]. After curing the thin films at 60°C for 2 h, PDMS prepolymer was applied to the edges of the membranes as a thick rim; after curing; this edge provided a support to use in manipulating the membranes on the Petri dishes. Typically, we used pieces of membrane that were 2 × 2 cm. The individual pieces of membrane were cut along the supports, peeled away from the posts, and placed on a coverglass with a few drops of ethanol; the ethanol wets the surface of the PDMS and allows the membrane with microfabricated holes to become flat and seal conformally to the coverglass. The membranes were used after evaporation of the ethanol. Importantly, it was necessary to render the apical surface of the membrane hydrophilic by brief exposure to an oxygen plasma in order to form

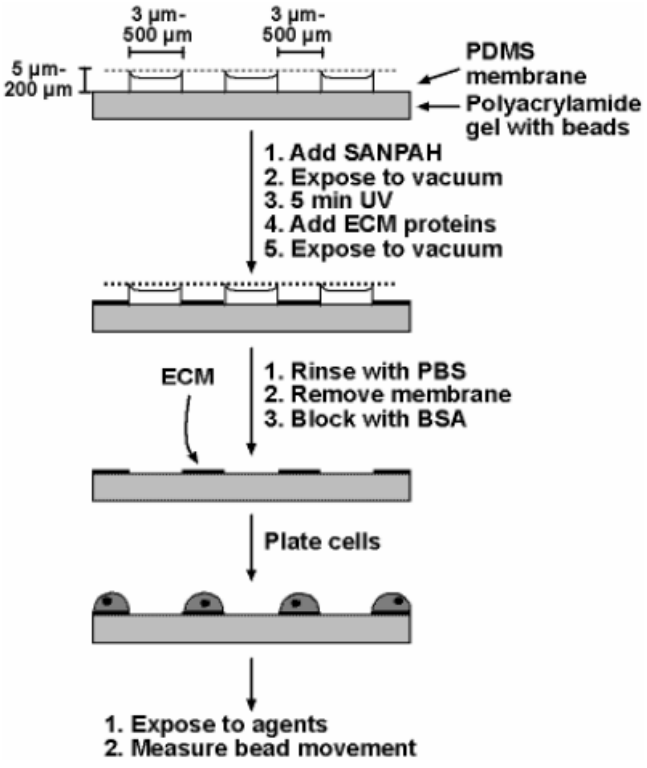

Fig. 1. Schematic illustration of the procedure used to pattern the attachment of ECM molecules on the surface of a flexible polyacrylamide gel. See Materials and Methods for a detailed description.

a reversible conformal seal with the polyacrylamide gel surface and, thus, prevent the collagen coating solution from leaking onto the surrounding surface of the gel. This was accomplished by oxidizing the apical surface of the membrane for 2 min in a plasma cleaner (Harrick Sci. Corp., Ossining, NY). The oxidized membranes were stored in deionized water until use [Delamarche et al., 1998].

Patterning ECM Proteins on Flexible Polyacrylamide Gels Using MEMPAT

Before placing the PDMS membrane on the gel, the gel was oriented with the layer of embedded fluorescent microbeads at the top. The film of water on the surface of the gel was gently removed by aspiration and the water on the membrane was removed by blotting with a piece of dry tissue and by applying a vacuum. The membrane was removed from the coverglass with a pair of forceps and was placed on the surface of the gel with the oxidized side of the PDMS contacting the gel (Fig. 1). In order to coat the gel with ECM, a few drops of 1 mM Sulfo-SANPAH (sulfosuccinimidyl-6- (4-azido-2-nitrophenyl-amino) hexanoate; Pierce, Rockford, IL) in 200 mM Hepes were added to activate the free surface of the gel that was exposed through the holes in the PDMS membrane in order to facilitate covalent attachment of proteins. The tightly apposed PDMS membrane and polyacrylamide gel were placed in a vacuum for 3 min to make sure SANPAH reached the gel surface. The system was then irradiated with the UV light of a sterile hood (254 nm wave length) for 5 min at a distance of 4–6 inches to link the SANPAH to the gel by photoactivation. The solution containing excess SANPAH was removed by aspiration, and the process of adding SANPAH and exposing to vacuum and UV light was repeated once (Initial Steps 1–3 in Fig. 1).

After the excess SANPAH was again removed by aspiration, type I collagen (0.2 mg/ml) was added to the membrane and the system was exposed to vacuum for 3 min to remove bubbles from the holes (Initial Steps 4,5 in Fig. 1). The surface of the gel was allowed to react with the collagen overnight at 4°C or for 2 h at 37°C. Excess collagen was removed by washing and the membrane was gently removed from the gel surface using a pair of forceps. A solution of serum-free medium containing 1% bovine serum albumin (BSA) was added for 30 min to block protein binding onto the newly exposed, uncoated surface of the polyacrylamide gel (Intermediate Steps 1–3 in Fig. 1). Cells were plated at high density (100,000 cells per membrane) to make sure that they adhered to the patterned areas; non-adherent cells were removed after 2 h by changing the medium. Attached cells were cultured overnight or for several hours before analysis. A schematic illustration of the method is shown in Figure 1.

Substrates for Analysis of Cell Spreading and Migration after Releasing Spatial Constraints

The protocol described above was modified for the study of cell spreading and movement into surrounding regions of the substrate after release of physical constraints to cell spreading. The polyacrylamide gel was first activated with SANPAH, in the absence of the membrane, and coated with type I collagen. After the gel was washed twice with PBS and the buffer was removed from the gel, the oxidized surface of the PDMS membrane with microfabricated holes was placed in direct contact with the collagen-coated surface of the gel. Serum-free medium containing 1% BSA was added for 30 min to block attachment of cells to the PDMS membrane. The cells were then plated for several hours, or overnight, until the cells attached to the collagen-coated surface exposed within the holes in the PDMS membrane. Using this method, both single cells and multiple cells could adhere to each island. The membrane was removed using a pair of forceps and changes in tractional forces associated with the movement of the cells onto the newly exposed areas of the collagen-coated gel were studied.

Traction Measurements

To determine the displacement field of the gel beneath individual adherent cells, images of the same region of the gel were taken at different times before or after experimental intervention. The position of the beads in the gel in the absence of traction was determined at the end of each experiment by releasing the cells by trypsinization; this tension-free image was used as a reference. The displacement field was determined by measuring changes in the position of the fluorescent beads when the reference image was compared with an image showing bead movements induced by adherent cells in the same portion of the gel (Final Steps 1,2 in Fig. 1). This was accomplished by identifying the coordinates of the peak of the cross-correlation function of each pair of small window areas ($6.5 \times 6.5\ \mu m^2$). The two-dimensional Fast Fourier Transform algorithm in MATLAB was used to calculate the correlation functions.

The traction field was calculated from the displacement field, implementing the solution described by Butler et al. [2002]. This calculation was based on the Boussinesq solution for the displacement field on the surface of a semi-infinite solid when the distribution of surface traction is known. Writing the displacements as a convolution of tractions and the kernel that maps tractions to displacements, and taking the Fourier transform of this relation, yield the solution for the traction field on the surface, when the surface displacement field and the gel elastic properties are known. The traction field was obtained by repetitive calculations from the displacement field using constrained Fourier Transform Traction cytometry that confined the tractions to the inside of a cell's boundary. The boundary conditions were: (1) zero traction outside of the cell-gel interfacial area and (2) the displacement field within the cell-gel interface that matched the experimentally observed displacements within the cell boundary. The root mean square (RMS) of tractions was calculated as the mean of traction stresses. The Poisson's ratio of the gel was assumed to be 0.48 [Wang et al., 2002].

RESULTS

ECM-coated adhesive islands of defined size, shape, and position on the micrometer scale were created by covalently coupling type I collagen to small regions of the surface of flexible polyacrylamide gels that were exposed through microengineered holes in a tightly apposed PDMS membrane (Fig. 1). When HASM cells were cultured on unpatterned collagen-coated polyacrylamide gels, they initially spread extensively (Fig. 2A) and eventually formed confluent monolayers (Fig. 2B) much as they do on conventional plastic culture dishes. In contrast, when the cells were cultured on 25- and 50-μm diameter collagen-coated circular islands, they exhibited small and large round forms, respectively (Fig. 2C,D). Similarly, when the cells were cultured on micropatterned gels containing 50- × 50-μm square adhesive islands, the cells remained confined to these squares (Fig. 2E) and conformed to their shape for at least 2 days in culture (Fig. 2F).

To explore whether the shape of the cells could influence the spatial distribution of the tension exerted on the substrate, cell tractions were calculated from measurements of the displacement fields of fluorescent beads within the subsurface of the gel in the presence of adherent cells. The displacement fields and traction force field (calculated from the displacement field) were determined by comparing the fluorescent images of the microbeads in the presence of living cells with images of the microbeads within the same region after the cells were removed by trypsinization (i.e., a stress-free condition) (Fig. 3). Under almost all conditions, the direction of the bead displacements was oriented toward the center of the cells.

Cells on the smallest islands (25-μm circles) displayed the least displacement of the microbeads and, hence, the lowest level of traction (Fig. 3, top). While larger bead displacements and tractions were observed in cells on both 50-μm diameter circles (Fig. 3, middle) and 50- × 50-μm squares (Fig. 3, bottom), the patterns of circles and squares differed. The greatest traction and bead displacements were observed along the outer edge (circumference) of the round cells on circular islands. Although there was no consistent orientation to where these stresses were applied, they appeared to colocalize with cell protrusions wherever they formed. In contrast, the greatest bead displacements and strongest tractional stresses appeared to consistently localize within the corner regions of square cells (Fig. 3, bottom). Cells in square islands also preferentially extend long cell processes from these corner regions (Figs. 2E,F, 3).

Past studies have demonstrated tight coupling between cell spreading and growth on micropatterned substrates [Singhvi et al., 1994; Chen et al., 1997], however, the role of cell-generated mechanical forces could not be determined. When the root-mean-square tractions beneath each cell were calculated for cells on all shapes and sizes of islands and then plotted as a function of projected cell areas, we observed a linear relationship between cell traction and cell spreading (Fig. 4). Thus, cell distortion produced by this micropatterning-based shape confinement method does produce a coordinated increase in cell contractile forces, as measured by traction exerted on the ECM substrate.

Treatment of the square HASM cells with the known contractile agonist, histamine (10 μM), also dem-

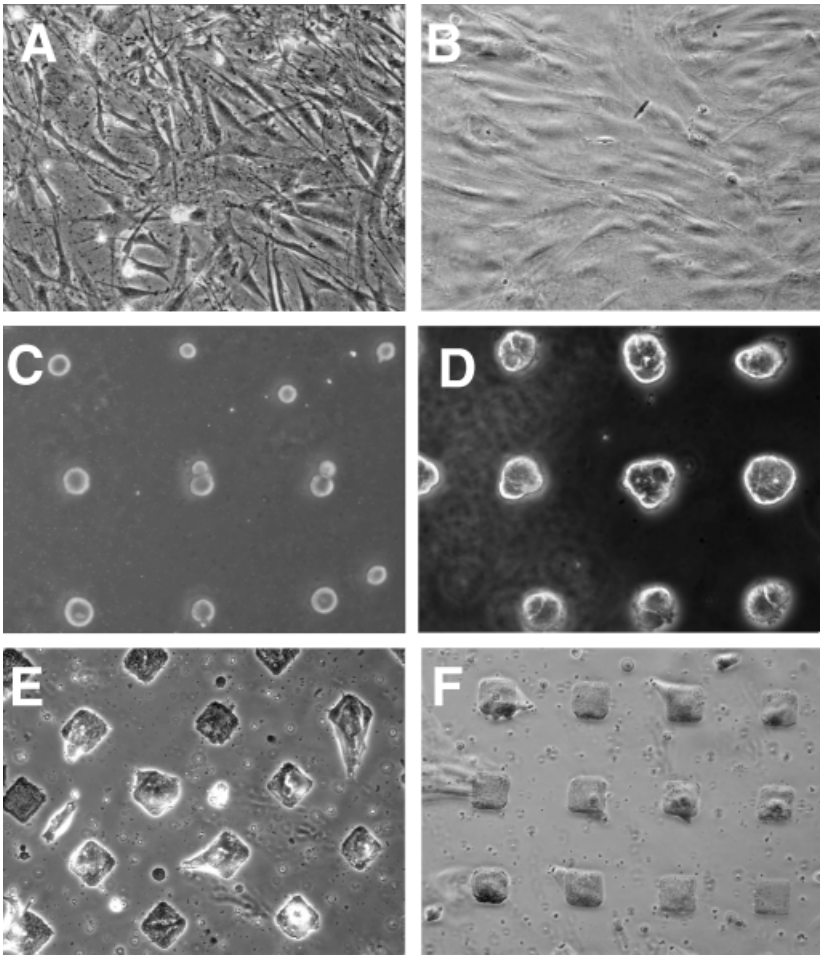

Fig. 2. Phase-contrast images of HASM cells cultured for 18 (**A, C–E**) or 48 (**B, F**) h on polyacrylamide gels on which collagen was either coated evenly across its surface (A, B) or limited to micrometer-sized islands of defined size, shape, and position (D–F). Cells spread and exhibited pleiomorphic forms on unpatterned gels (A), resulting in formation of a confluent monolayer by 48 h of culture (B). In contrast, cells cultured on similarly coated circular adhesive islands, 25-μm (C) or 50-μm (D) diameter, or on square islands with 50-μm edges (E, F), remained constrained to the size and shape of the islands for the entire period of study.

onstrated that active cell contraction can be visualized with this technique (Fig. 3, bottom, far right). Stimulating the cell contraction clearly increased the traction stresses relative to those of the untreated cells (RMS traction increased by 32 Pa [36%] from the baseline value of 88 Pa) and, again, the stresses were exerted preferentially in the corners of these square cells (the greatest net increase of local traction was about 100 Pa at the bottom corner, Fig. 3, bottom, far right). In other words, the shape of the cell governed *where* these increased forces were located and directed. Interestingly, the increase in traction due to histamine stimulation was not equal in all corners. In fact, the regions that exerted the most traction in the resting cells exhibited the least net increase in traction after agonist stimulation (Fig. 3, bottom right vs. far right).

Using the approach of overlying the membrane on the pre-coated gel substrate, we were able to study cell spreading after the membrane was peeled off. We found that the cells that were originally limited to the 50-μm square islands (Fig. 5A) extended out long processes over the first 6 to 8 h (Fig. 5B) and onto the surrounding collagen-coated gel surface over the next day (Fig. 5C). Traction force analysis of cells that were allowed to spread for 6 h after membrane removal (Fig. 5D) showed that the greatest bead displacements (Fig. 5E) and traction stresses (Fig. 5F) were concentrated beneath the cell's long protrusions that extended onto the surrounding ECM substrate, although relatively large tractions also occurred at the periphery of the cell body. Similar results also were obtained with cells plated on 50-μm-diameter circles (not shown).

DISCUSSION

It is known that cell-generated tensional forces play an important role in cell shape control [Chicurel et al., 1998] and that the shape of a cell can influence its growth and function [Singhvi et al., 1994; Chen et al., 1997]. Some of the best experimental evidence in support of shape-dependent growth control comes from studies with micropatterned substrates that spatially confine cells to the size and shape of ECM-coated adhesive islands that are separated by non-adhesive regions. Various labora-

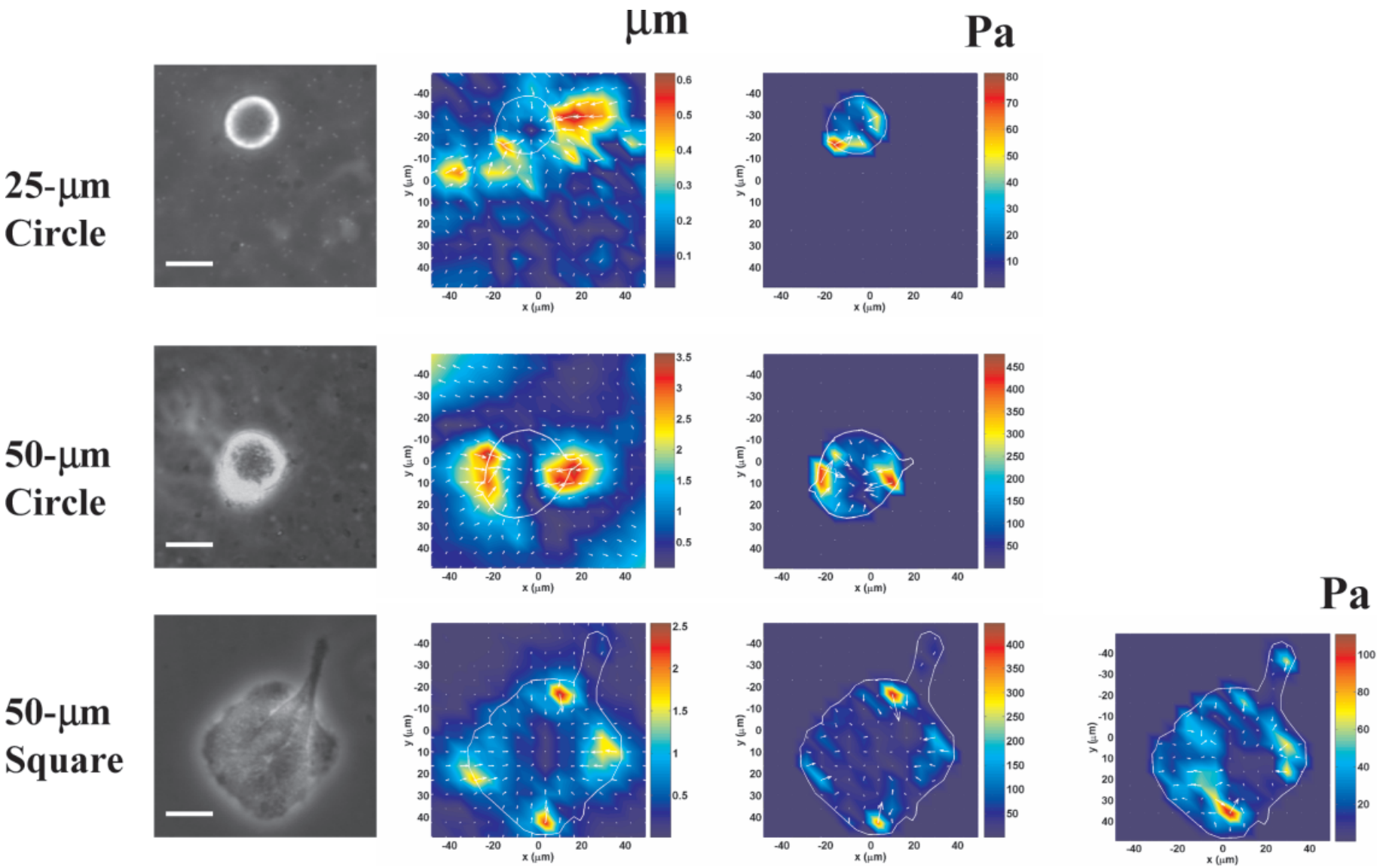

Fig. 3. Phase contrast images of cells cultured on round and square micropatterned adhesive islands (**left column**) and maps of their displacement fields (**middle column**) and traction fields (**right and far right columns**). *Arrows* indicate directions of the bead displacements (middle) and associated traction stresses (right, far right). The color scale indicates the magnitudes of the displacements (in μm) and of the tractions (in Pa). The two traction field maps shown in the bottom row (right and far right) indicate the same cell on a square island in the absence (RMS traction = 88 Pa) and presence of the contractile agonist, histamine (10 μM for 2 min). The traction field at the far right shows the net change in traction (RMS traction = 32 Pa) in the histamine-treated cell relative to the untreated cell. Note that the greatest displacement and tractions preferentially concentrate in the corner regions of the square cell; a long protrusion can be observed to extend upward just to the right of the top corner of this cell. Scale bar = 20 μm.

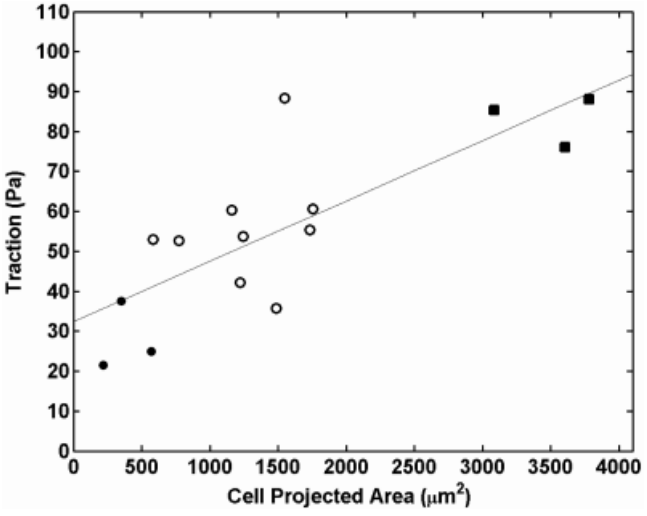

Fig. 4. Relationship between mean cell traction and cell spreading within cells cultured on micrometer-sized adhesive islands of different size and shape. The root mean square traction and the projected area of each cell were measured 14–18 h after plating onto micropatterned polyacrylamide gel substrates. Closed squares, 50 × 50 μm square islands; closed circles, 25-μm diameter circular islands; open circles, 50-μm diameter circular islands. The slope of the linear regression line was 0.015 Pa/μm^2 and the intercept was 32.4 Pa; r = 0.79.

tories have used this method to show that cell proliferation generally increases as the island area is increased and cell spreading is promoted [O'Neill et al., 1986; Singhvi et al., 1994; Chen et al., 1997]. These effects of cell shape on growth have been proposed to result from changes in the cellular mechanical force balance [Singhvi et al., 1994; Chen et al., 1997; Chicurel et al., 1998] based on the notion that ECM islands of increasing area may resist greater levels of cell traction and thereby increase isometric tension inside the cell. This is important because cytoskeletal tension has been shown to be critical for cell cycle progression [Huang et al., 1998]. However, it has not been possible to determine directly the contribution of cell tension to this form of behavior control.

In a recent study, distortion of microscopic posts was used as a strain gauge to calculate the local contact forces generated by adherent cells at individual focal adhesions [Balaban et al., 2001]. Other studies quantitate cell tractional forces beneath large regions of single cells with microelectromechanical (MEMS) devices [Galbraith and Sheetz, 1996] or by using flexible silicon rubber membranes [Lee et al., 1994] or polyacrylamide gels [Dembo and Wang, 1999] that contain microbeads to permit quantitation of displacement and traction fields beneath individual cells. In contrast, in the present study, we set out to quantitate tractional forces beneath individual cells whose size and shape were highly constrained by combining two previously described techniques: MEMPAT and traction force microscopy.

The successful application of this combined approach relied on the formation of a tight seal between the PDMS and the apical surface of the gel. When the seal between the PDMS membrane and gel surface was not tight, solutions leaked and no detectable patterns formed. Since the gel is hydrophilic and the PDMS membrane is hydrophobic, the key advance necessary to make this method possible was the addition of a plasma treatment step to make the membrane's surface hydrophilic. The seal between the membrane and gel surface was significantly improved by addition of this step and adhesive islands could be formed with high fidelity (Figs. 2, 3).

Cell Tension and Cell Spreading

Using this method, we were able to clearly quantitate displacement and traction fields beneath individual micropatterned cells. In contrast to the method in which distortion of microfabricated flexible posts is used as a strain gauge and local contact forces that are more than 3 μm apart can be reliably determined [Balaban et al., 2001], our traction calculations are limited only by the resolution (about 0.4 μm) of the displacement measurements [Butler et al., 2002; Wang et al., 2002]. Our studies demonstrated that both the size and shape of the cell feed back to influence cell traction. In general, the mean cell traction increased in parallel as cell spreading was promoted. Thus, this quantitative analysis confirms that spread cells that exhibit an enhanced ability to enter S phase and proliferate [Singhvi et al., 1994; Chen et al., 1997] do experience increased cell tension. This is consistent with a recent finding that shows that the rigidity of the substrate regulates growth and apoptosis of normal cells, possibly through controlling cell traction and spreading [Wang et al., 2000]. Elevated tension in the cytoskeleton may, in turn, promote cell cycle progression by down-modulating the cdk inhibitor, p27, and up-regulating the growth promoter, cyclin D1 [Huang et al., 1998].

Traction Concentration at Corners

Importantly, the size and geometry of the adhesive islands also influenced the spatial distribution of tractional stresses. For example, while round cells did not exhibit any consistent pattern of stress application, cells on square islands consistently exerted their greatest level of traction in regions localized at each of the four corners of the cell. However, the magnitudes of the tractions were not evenly distributed at each corner. In migrating fibroblasts, strong tractions appear to occur at small-sized and nascent focal adhesions [Beningo et al., 2001] and, thus, the local differences in traction distribution that we observed might be related to differences in focal adhe-

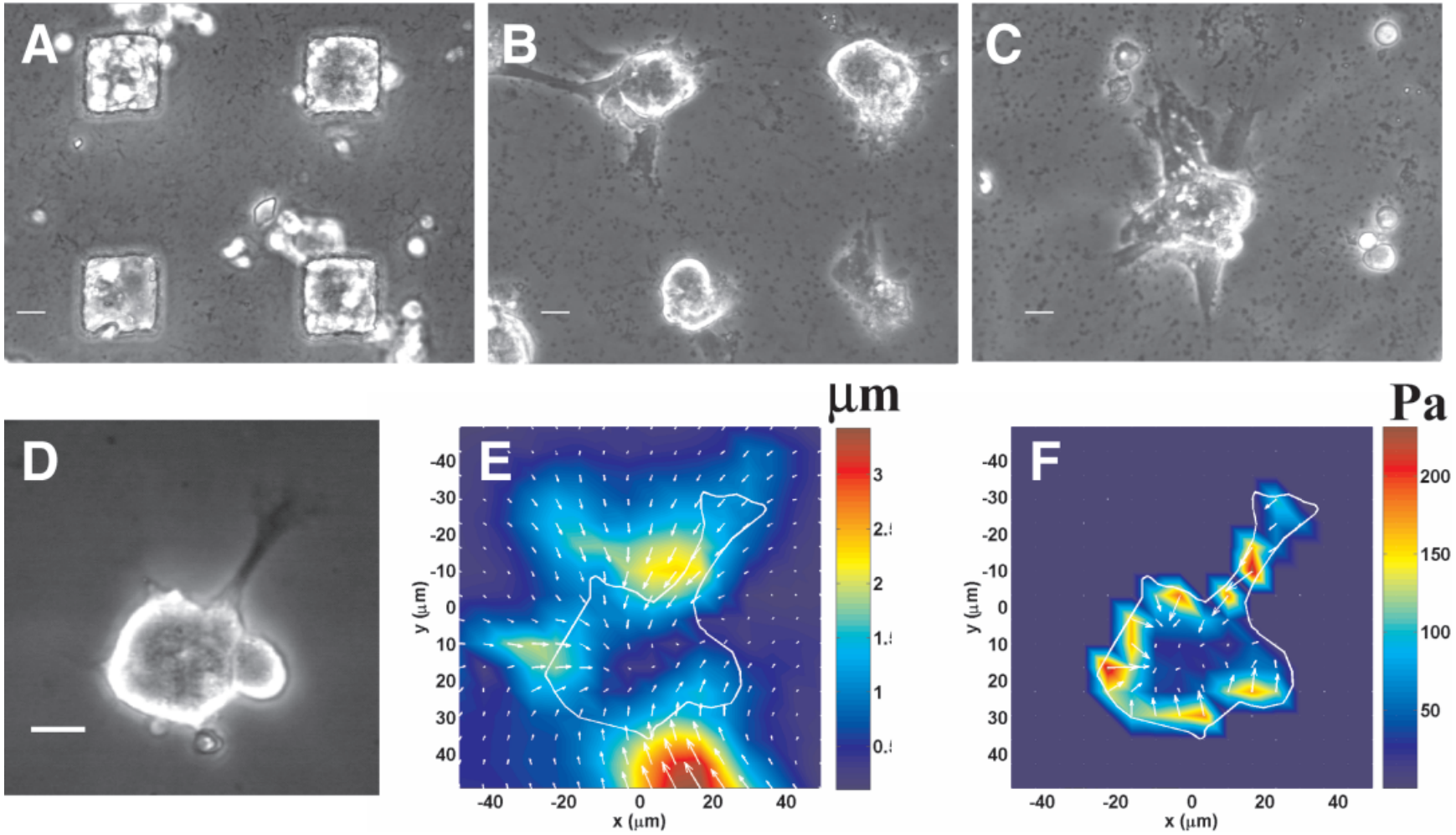

Fig. 5. Cell spreading onto exposed regions of the ECM surface after release of shape confinement within 50-μm square holes within a PDMS membrane that masked the collagen-coated surface of a polyacrylamide gel (A–C) and related traction force analysis (D–F). **A:** Cells' adhesion to the gel surface was restricted to the square openings in the PDMS covering membrane when it remained attached to the gel surface. **B:** Cells extended long processes onto the exposed surface of the collagen-coated gel within 6–8 h after the membrane was peeled off. **C:** Cells spread and migrated onto the surrounding surface of the gel within one day after the membrane was removed. **D:** Phase contrast image of two cells adherent to a square region of the gel surface 6 h after the PDMS membrane was removed. Note the long cell protrusion oriented towards the top right of the view and a small round cell is attached to the top right corner of the large square cell that has small protrusions at other corners. **E:** Directions (*arrows*) and magnitudes (colors) of the displacement fields of this cell. **F:** Directions (*arrows*) and magnitudes (colors) of the traction field. Scale bar = 20 μm.

sion dynamics. Alternatively, the difference in traction amplitudes might reflect the size of the focal adhesions since the magnitude of tractions correlates with focal adhesion size in spread, non-migrating fibroblasts [Balaban et al., 2001]. Nevertheless, the adhesion sites in the corners of the square cells appeared to be physiological points of tension application since cells exerted tension on these same localized adhesions when stimulated with the contractile agonist, histamine. The preexisting ECM adhesion points did not, however, all increase their tractions to a similar level when stimulated with histamine. Adhesions that exhibited the lowest level of traction in the unstimulated state appeared to display the greatest response to histamine stimulation (Fig. 3, bottom). It is possible that each adhesion site may be limited in terms of the maximal amount of stress that can be exerted on it and, thus, the sites that are already greatly stressed before histamine addition may already be near their saturation point. Alternatively, increased tension application to new sites may shift the cellular force balance and result in a redistribution of forces throughout the entire cell. Regardless of the mechanism, these results indicate that this technique can be used to study the contractile response within individual cells.

The finding that cell tractional forces are concentrated within the corners of square cells is consistent with the recent finding that cells preferentially form focal adhesions containing vinculin in their corners when cultured on square adhesive islands [Parker et al., 2000]. Although the reason for this remains unclear, this polarized distribution of focal adhesions and traction application (as measured here) appears to correlate with localized formation of cell protrusions (i.e., lamellipodia, filopodia, and microspikes), which extend outward from these same corner regions in square cells [Parker et al., 2000] (Figs. 2E,F; 3, bottom; 5). Importantly, round cells also appeared to concentrate their tractional stresses in localized regions where cell protrusions formed. Analysis of unpatterned cells using traction force microscopy by others similarly demonstrated tractional forces in regions near where migrating cells extend lamellipodia [Dembo and Wang, 1999]. Taken together, these results suggest that spatial confinement of cells may influence the direction in which cells will extend processes that lead cell migration at least in part by influencing where cells exert their tractional forces on the ECM substrate.

This hypothesis for traction-dependent steering of cell movement is supported by studies in which tractional forces were quantitated beneath cells that were released from spatial confinement by pulling off the PDMS membrane and thereby permitting cell spreading and movement onto the surrounding surface of the ECM-coated gel (Fig. 5). These studies once again confirmed that cells appear to exert their greatest traction at sites where they extend new processes that drive cell migration. Thus, the new method described here may be especially useful for analyzing the biophysical basis of directional control of cell migration in the future.

We previously reported that cell stiffness (defined as the ratio of shear stress to shear strain) is tightly coupled to cell spreading [Wang and Ingber, 1994, 1995]: the larger the projected cell area, the greater the stiffness. In the present study, we found that the root mean square traction also increased with cell spreading, confirming that cell stiffness is tightly coupled to the level of isometric tension within the cell. Given that cell tractional forces originate from cytoskeletal contractile forces [Wang et al., 2002], these results are consistent with the finding that cell stiffness increases with cytoskeletal pre-stress (the level of pre-existing tensional stresses in the cytoskeleton prior to force application) [Wang et al., 2001]. In past studies, it has been found that the total area of focal adhesions beneath a single cell increases with cell spreading area [Davies et al., 1994]. Thus, the magnitude of cell traction may increase with the total focal adhesion area as well. This is consistent with the finding that local contact forces increase with the area of individual focal adhesions [Balaban et al., 2001]. Our results are not inconsistent with those of Beningo et al. [2001] who have shown that strongest tractions occur at nascent small focal adhesions since our tractions are values averaged over the whole cell whereas theirs are local transient tractions at the leading edge of migrating cells. Finally, tension has been shown to promote focal adhesion formation and recent studies suggest that cell spreading may stimulate myosin light chain phosphorylation (T. Polte and D.E. Ingber, unpublished results), thereby increasing cytoskeletal tension generation directly. Thus, spread cells may produce larger and more numerous focal adhesions because they generate increased tractional forces.

In summary, we have described a new method in which the shape of individual cultured cells can be varied independently under conditions in which the magnitude and distribution of cell tractional stresses can be quantified. This approach of micropatterning cell shape on flexible gels allows us, for the first time, to directly determine how cell-generated mechanical forces contribute to cell shape-dependent control of complex behaviors, including growth, contractility, and migration of individual cells and groups of cells.

ACKNOWLEDGMENTS

We thank Jianxin Chen, Zhuangli Liang, and Iva M. Tolić-Nørrelykke for assistance. We thank Dr. R. Panettieri for HASM cells. This work was supported by NASA and NIH grants: NAG2-1509 (N.W.), HL65371

& HL33009 (N.W.), GM30367 (G.M.W.), CA45548 (D.E.I.), and by Harvard's MRSEC shared facilities funded by NSF DMR-9400396.

REFERENCES

Baill M, Yan L, Whitesides GM, Condeelis JS, Segall JE. 1998. Regulation of protrusion shape and adhesion to the substratum during chemotactic responses of mammalian carcinoma cells. Exp Cell Res. 241:285–99.

Balaban NQ, Schwarz US, Riveline D, Goichberg P, Tzur G, Sabanay I, Mahalu D, Safran S, Bershadsky A, Addadi L, Geiger, B. 2001. Force and focal adhesion assembly: a close relationship studied using elastic micropatterned substrates. Nat Cell Biol 3:466–472.

Beningo K, Dembo M, Kaverina I, Small V, Wang, Y.-L. 2001. Nascent focal adhesions are responsible for the generation of strong propulsive forces in migrating fibroblasts. J Cell Biol 153:881–888.

Butler JP, Tolić-Nørrelykke IM, Fabry B, Fredberg, JJ. 2002. Traction fields, moments, and strain energy that cells exert on their surroundings. Am J Physiol Cell 282:C595–C605.

Chen CS, Mrksich M, Huang S, Whitesides GM, Ingber DE. 1997. Geometric control of cell life and death. Science 276:1425–1428.

Chicurel ME, Chen CS, Ingber DE. 1998. Cellular control lies in the balance of forces. Curr Opin Cell Biol 10:232–239.

Davies PF, Robotewskyj A, Griem ML. 1994. Endothelia cell adhesion in real time. J Clin Invest 93:2031–2038.

Dembo M, Wang Y-L. 1999. Stresses at the cell-to-substrate interface during locomotion of fibroblasts. Biophys J 76:2307–2316.

Delamarche E, Bernard A, Schmid H, Michel B, Biebuyck H. 1997. Patterned delivery of immunoglobulins to surface using microfluidic networks. Science 276:779–781.

Dike L., Chen CS, Mrkisch M, Tien J, Whitesides GM, Ingber DE. 1999. Geometric control of switching between growth, apoptosis, and differentiation during angiogenesis using micropatterned substrates. In Vitro Cell Dev Biol 35:441–448.

Duffy DC, Jackman RJ, Vaeth K, Jensen KF, Whitesides GM. 1999. Patterning electroluminescent materials with feature sizes as small as 5 mm using elastomeric membranes as masks for dry lift-off. Adv Mater 11:546–552.

Galbraith CG, Sheetz MP. 1997. Forces on adhesive contacts affect cell function. Proc Nat Acad Sci USA 94:9114–9118.

Huang S, Chen CS, Ingber, DE. 1998. Control of cyclin D1, $p27^{Kip1}$, and cell cycle progression in human capillary endothelial cells by cell shape and cytoskeletal tension. Mol Biol Cell 9:3179–3193.

Jackman RJ, Duffy DC. Cherniavskaya O, Whitesides GM. 1999. Using elastomeric membranes as dry resists and for dry lift-off. Langmuir 15:2973–2984.

Lee J, Lenord M, Oliver TN, Ishihara A, Jacobson K. Traction forces generated by locomoting keratocytes. 1994. J Cell Biol 127: 1957–1964.

O'Neill C, Jordan P, Ireland G. 1986. Evidence for two distinct mechanisms of anchorage stimulation in freshly explanted and 3T3 Swiss mouse fibroblasts. Cell 44:489–496.

Ostuni E, Kane R, Chen CS, Ingber DE, Whitesides GM. 2000. Patterning mammalian cells using elastomeric membranes. Langmuir 16:7811–7819.

Panettieri RA, Murray RK, DePalo LR, Yadvish RA, Kotlikoff MI. 1989. A human airway smooth muscle cell line that retains physiological responsiveness. Am J Physiol 256:C329–C335.

Parker KK, Brock AL, Brangwynee C, Ingber DE. 2000. Extracellular matrix geometry and mechanics direct lamellipodia extension. Mol Biol Cell 11:86a.

Pelham RJ, Wang Y-L. 1997. Cell locomotion and focal adhesions are regulated by substrate flexibility. Proc Natl Acad Sci USA 94:13661–13665.

Qin D, Xia Y, Whitesides GM. 1996. Rapid prototyping of complex structures with feature sizes larger than 20 mm. Adv Mater 8:917–919.

Singhvi RA, Kumar A, Lopez G, Stephanopoulos GN, Wang DIC, Whitesides GM, Ingber DE. 1994. Engineering cell shape and function. Science 264:696–698.

Wang H-B, Dembo M, Wang Y-L. 2000. Substrate flexibility regulates growth and apoptosis of normal but not transformed cells. Am J Physiol Cell Physiol 279:C1345–1350.

Wang N, Ingber DE. 1994. Control of cytoskeletal mechanics by extracellular matrix, cell shape, and cytoskeletal tension. Biophys J 66:1281–1289.

Wang N, Ingber DE. 1995. Probing transmembrane mechanical coupling and cytomechanics using magnetic twisting cytometry. Biochem Cell Biol 73:327–335.

Wang N, Naruse K, Stamenović D, Fredberg, JJ, Mijailovich SM, Tolić-Nørrelykke IM, Polte T, Mannix R, Ingber DE. 2001. Mechanical behavior of living cells consistent with the tensegrity model. Proc Natl Acad Sci USA 98:7765–7770.

Wang N, Tolić-Nørrelykke IM, Chen J, Majailovich SM, Butler JP, Fredberg JJ, Stamenović, D. 2002. Cell prestress. I. Stiffness and prestress are closely associated in adherent contractile cells. Am J Physiol Cell 282:C606–C616.